Available online www.jocpr.com

Journal of Chemical and Pharmaceutical Research, 2016, 8(1):279-286

Research Article

ISSN : 0975-7384
CODEN(USA) : JCPRC5

Crystal structure and DFT calculations of 4,5-dichloropyridazin-3-(2*H*)-one

Silva-Júnior E. F.[1,2], Silva D. L.[1], Santos-Júnior P. F. S.[1], Nascimento I. J. S.[1], Silva S. W. D.[3], Balliano T. L.[3], Aquino T. M.[1,2] and Araújo-Júnior J. X.*[1,2]

[1]*Laboratory of Medicinal Chemistry (LMC), Federal University of Alagoas, Av Lourival Melo Mota, s / n, Tabuleiro dos Martins, Maceio – Alagoas, Brazil*
[2]*Chemistry and Biotechnology Institute, Federal University of Alagoas, Av Lourival Melo Mota, s / n, Tabuleiro dos Martins, Maceio – Alagoas, Brazil*
[3]*Laboratory of Crystallography, Federal University of Alagoas, Av Lourival Melo Mota, s / n, Tabuleiro dos Martins, Maceio, Alagoas, Brazil*

ABSTRACT

The title compound, 4,5-Dichloropyridazin-3-(2H)-one, has been characterized using ¹H and ¹³C NMR spectroscopic and crystallographic techniques. The compound crystal in the monoclinic space group $P2_{1/c}$ with a= 5.22 (1) Å, b= 9.08 (2) Å, c= 12.97 (3) Å, α=γ= 90.0 (0)°, β= 100.47 (2)° and D_x= 1.808 g/cm^3, respectively. The structure of the compound has also been examined by using quantum chemical methods. The molecular geometry and vibrational frequencies of monomeric and dimeric forms of the title compound in the ground state have been calculated using the Density Functional Theory (DFT) and B3LYP/6-31G(d,p) as basis set. The calculated results show that the optimized geometry and the theoretical vibration frequencies of the dimeric form are good agreement with experimental data. In addition, MEP map, HOMO, LUMO, energy gap ($\Delta E= E_{HOMO}-E_{LUMO}$), electronegativity (x), hardness (η), softness (ζ), and electronegativity index (ψ) of the 4,5-dichloropyridazin-3-(2H)-one were performed at B3LYP/6-31G(d,p) level of theory.

Key words: DFT calculations, B3LYP/6-31G(d,p), Theoretical study, Pyridazine ring, X-ray crystallography

---

INTRODUCTION

The six-membered nitrogenated aromatic ring molecules, such as diazines have been very studied [1]. Diazines, such as pyridazine, represent an important class of active molecules [2,3]. These are characterized by the presence of nitrogen atoms with electron lone pairs which are able to interact with acids in gas phase, solution or condensed phase [2]. It posses two different kinds of proton-acceptor sites, one is the ring π cloud and another is the lone pairs on the nitrogen atoms [1].

Currently, the development of computational chemistry has contributed to the research of theoretical modelling of drug design and functional material design in a positive way over the past decade [4]. In addition, it has become possible to propose important physico-chemical properties of biological and chemical systems by diverse computational techniques [4]. Recently, Density Functional Theory (DFT) has been a great tool on theoretical modelling [4,5]. Calculating many molecular properties with comparable accuracies to traditional correlated *ab initio* methods with more plausible computational costs has become possible with the development of better exchange-correlation functional [4]. The studies in literature showed that the DFT has a perfect accuracy in reproducing the experimental values of in geometry, dipole moment and vibrational frequency [1,3,4].

In this manuscript, the 4,5-dichloropyridazin-3-(2H)-one was re-synthesized according to reference [6] and characterized by ¹H and ¹³C NMR, single crystal X-ray and DFT methods. Hydrogen bond geometry of the molecule

was determined using X-ray diffractometer. Furthermore, the properties of structural geometry, molecular electrostatic potential map (MEP), frontier orbitals (HOMO and LUMO), energy gap ($\Delta E = E_{HOMO}-E_{LUMO}$), electronegativity ($x$), hardness ($\eta$), softness ($\zeta$), and electronegativity index (ψ) of the 4,5-dichloropyridazin-3-(2H)-one were calculated at B3LYP/6-31G(d,p) level of theory.

EXPERIMENTAL SECTION

General

All reagents were commercial grade and purified according to the established procedures. ^{1}H and ^{13}C NMR were obtained using a Bruker® Avance DRX Spectrometer on 400 MHz using tetramethylsilane (TMS) as internal standard. All chemical shift values were recorded as δ (ppm), the peaks are presented as *s* (singlet) and *br* (broad singlet). The reactions were monitored by thin layer chromatography (Merck®, silica gel, type 60, 0.25 mm).

Synthesis

Hydrazine sulphate **(1)** (305 mg, 2.35 mmol) and 3,4-Dichloro-5-hydroxy-5*H*-furan-2-one **(2)** (419 mg, 2.48 mmol) and sodium acetate (212 mg, 2.58 mmol) were added into a round bottom-flask with water (10 mL). The mixture was stirred at 100 ºC, during 4 hours. After the reaction to finish, the solvent was removed under reduced pressure and a filtration was performed. The residual solid was recrystallized from ethanol to afford the compound **(3),** as a colourless powder (216 mg, 67% (Scheme 1).

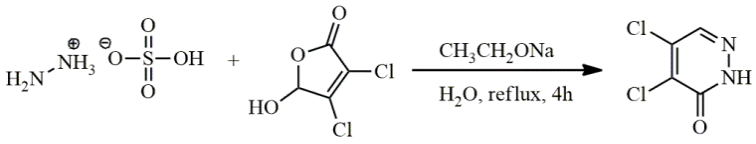

(1) **(2)** **(3)**

Scheme 1. Synthetic route for the 4, 5-dichloropyridazin-3(2*H*)-one obtainment

Computational Details

All calculations were performed using the *WaveFunction Spartan*® program, version 1.1.0 developed by The Design Center, Pittsburgh, 1991-2011[7]. Starting geometries of compound were taken from X-ray refinement data. The molecular structure of the compound in the ground state was optimized using B3LYP/6-31G(d,p) level of the theory [2,4,5,7]. In Density Functional Theory (DFT) calculations, hybrid functional were also used, the Becke's three parameter functional (B3) with defines the exchange functional as the linear combination of *Hartree-Fock*, local and gradient - corrected exchange terms [4,8,10]. For the compound, vibration frequencies were calculated using DFT/B3LYP with 6-31G(d,p) basis set [2,4,8,9]. In addition, MEP map, highest occupied molecular orbital (HOMO), lowest unoccupied molecular orbital (LUMO), energy gap ($\Delta E = E_{HOMO}-E_{LUMO}$), electronegativity ($x$), hardness ($\eta$), softness ($\zeta$), and electronegativity index (ψ) of the 4,5-dichloropyridazin-3-(2H)-one were calculated using B3LYP/6-31G(d,p) level of the theory [4,10,11]. Finally, all data results were analyzed by statistical methods, correlation index (r^2) and linear regression, using *Minitab*®, version 17.0, trial license.

X-Ray Diffraction Crystallography

Pyridazine crystals were grown by slow evaporation method from a saturated hexane solution of stoichiometric quantities of pyridazine and tetrahydrofuran (THF). The evaporation took place at constant temperature of 25 ºC.

Through crystallochemical studies about the compound **(3)** was possible to determine the structure and conformational analysis. For this, was selected a sample from this crystal and fixed in the head of goniometric of the automatic diffractometer Kappa CCD of the Enraf-Nonius [14], equipment of x-ray diffraction used for to perform the intensity collections of the diffracted ray-x beams in room temperature (T= 298K). Then, the data were collected and processed and the structure was determined using the WingX v1.80.05 [15]. Using the electronic density map, were analyzed the distances and interatomic angles, providing the localization of the atoms (including classical hydrogen interactions), the rest of the hydrogen were positioned considering the geometry of the others attached atoms. After the identification of all atoms, was used the Ortep-3 v.2.02 [16] for to obtain the representation of the compound. Through the PovRay v3.6 [17] program, was possible to visualize the identification of the atoms, as well their thermal vibrations ellipsoids to 50% of probability. Furthermore, was used the Mercury v2.2 [18] program for analysis of the crystal packing and hydrogen interactions.

RESULTS AND DISCUSSION

Synthesis

The compound **(3)** was obtained with satisfactory yield (95 %), superior than some methodologies found in literature. ^{1}H NMR (400 MHz, $DMSO_{d\text{-}6}$): 8.04 (*s*, 1H, N=CH) and 13.67 (*br*, 1H, C-NH). ^{13}C NMR (100 MHz, $DMSO_{d\text{-}6}$): 133.70 (C-Cl1), 137.08 (C-Cl2), 137.28 (C=N), 157,46 (C=O).

Crystallographic Study

The title compound **(3)** crystallizes in the monoclinic space group $P2_{1/c}$, an Ortep view of **(3)** is shown in Figure 1, and crystal data, data collection and refinement details for this compound are shown in Table 1. The compound in study presented a six member ring, being 4 carbon and 2 nitrogen atoms.

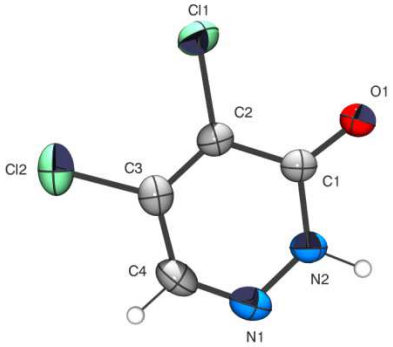

Figure 1. Ortep view for the monomeric form of the title compound and atom numbering schemes

The C1, C2, and C3 atoms show, respectively, a double bond with oxygen and two single bonds with chloride atoms. The presence of the N2 atom in this ring show important role in the formation of classical hydrogen bonds, together with the oxygen atom (O1) attached to C1 and which perform a classical hydrogen bond as secondary bound.

Table 1. Crystal data, data collection and refinement detail for the title compound

Data for the crystal		
Molecular formula	$C_4 H_2 Cl_2 N_2 O$	
Molecular Mass	164.98	
Temperature	293 K	
Wavelength [Kα(Mo)]	0.71073 Å	
Crystal system	Monoclinic	
Spatial group	$P2_1/c$	
Unitary cell dimension	a = 5.2275(1) Å b = 9.0849(2) Å c = 12.9770(3) Å α = γ = 90.0º(0) β = 100.471º(2)	
Volume	606.03(2) $Å^3$	
Z (molecules by unitary cell)	4	
Density (calculated)	1.808 g/cm^3	
Absorption coefficient	Mu(MoKa) [/mm]	0.974 mm^{-1}
F(000)	328	
Gap of θ for the collection	3.9 to 28.1º	
Collected reflection	3672	
Independent reflections	1229	
Observed reflections	978	
R intern	0.0425	
Nº of refined parameters	82	
Goof (S)	1.1510	
Index $R_{obs.}$ [I >2σ(I)]	0.0352	
Index $R_{all.}$	0.0481	
Index R for all data	$wR2_{\_all}$ = 0.113	$wR2_{\_obs}$ = 0.107

The molecules of each unitary cell of the compound presented classical hydrogen interactions, [N2−H1N2···O1], with distance and angle equal to 1.894 Å and 166.65º, respectively (Figure 2). These interactions between molecular pairs strengthen the stability of the crystal arrangement. As observed in Figure 2, in this rearrangement were localized secondary hydrogen interactions, [C4−H4···O1], showing 2.378 Å and 171.18º for the distance and angle bonds, respectively (Table 3). From these interactions, is maintained a stable connection between adjacent molecules inside the unitary cell.

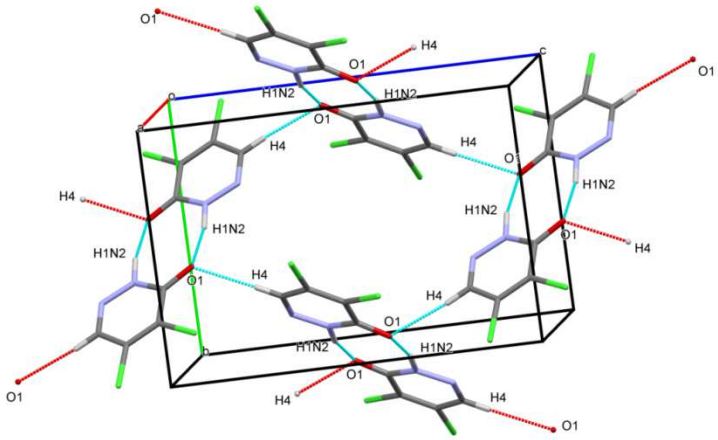

Figure 2. Packing diagram of the title compound

Optimized Geometry

The optimized parameters (bond lengths, bond angles, and dihedral angles) of monomer and dimer forms of the title compound were obtained at B3LYP level with the 6-31G(d,p) basis set and listed with the experimental values in Table 2.

Table 2. Selected molecular structure parameters

Parameters	Experimental (±SD)*	B3LYP/6-31G(d,p)	
		Monomer	Dimer
Bond lengths (Å)			
Cl1-C2	1.711(2)	1.720	1.721
Cl2-C3	1.711(2)	1.738	1.736
O1-C1	1.237(2)	1.218	1.235
N1-N2	1.345(2)	1.338	1.336
N1-C4	1.296(3)	1.302	1.305
N2-C1	1.364(2)	1.401	1.386
N2-H1N2	0.9700	1.014	1.034
C1-C2	1.452(3)	1.473	1.386
C2-C3	1.357(3)	1.367	1.369
C3-C4	1.413(3)	1.434	1.430
N2-H1···O1A	1.894	-	1.807
Bond angles (º)			
N2-N1-C4	116.33(18)	116.51	117.12
N1-N2-C1	127.42(17)	129.15	127.87
N1-N2-H1N2	114.00	115.25	115.47
C1-N2-H1N2	118.00	115.60	116.66
N2-C1-C2	114.37(17)	112.14	113.71
O1-C1-N2	120.98(18)	121.21	121.71
O1-C1-C2	124.65(18)	126.65	124.58
C1-C2-C3	119.08(19)	119.64	119.15
Cl1-C2-C1	117.05(16)	116.34	116.87
Cl1-C2-C3	123.87(16)	124.01	123.98
Cl2-C3-C2	121.98(16)	122.92	122.87
Cl2-C3-C4	118.93(15)	117.43	117.82
C2-C3-C4	119.09(19)	119.64	119.31
N1-C4-C3	123.67(19)	122.92	122.83
N1-C4-H4	118.00	116.77	116.78
Dihedral angles (º)			
C4-N1-N2-C1	2.3(3)	0.0	0.0
N2-N1-C4-C3	-0.2(3)	0.0	0.0
N1-N2-C1-O1	177.44(19)	180.0	180.0
N1-N2-C1-C2	-2.5(3)	0.0	0.0
O1-C1-C2-C3	-179.22(19)	180.0	180.0
N2-C1-C2-Cl1	-179.84(14)	180.0	180.0
O1-C1-C2-Cl1	0.3(3)	0.0	0.0
N2-C1-C2-C3	0.7(3)	0.0	0.0
Cl1-C2-C3-C4	-178.41(15)	180.0	180.0
C1-C2-C3-Cl2	-179.66(15)	180.0	180.0
Cl1-C2-C3-Cl2	0.9(3)	0.0	0.0
C1-C2-C3-C4	1.0(3)	0.0	0.0
Cl2-C3-C4-N1	179.31(17)	180.0	180.0
C2-C3-C4-N1	-1.4(3)	0.0	0.0

**: Standard-deviation.*

The optimized molecular structures for monomer and dimer forms of this compound are shown in Figure 3 (a) and (b), respectively. In table 3, O1···H1N2 and O1···H4C4 experimental values are shown in Å.

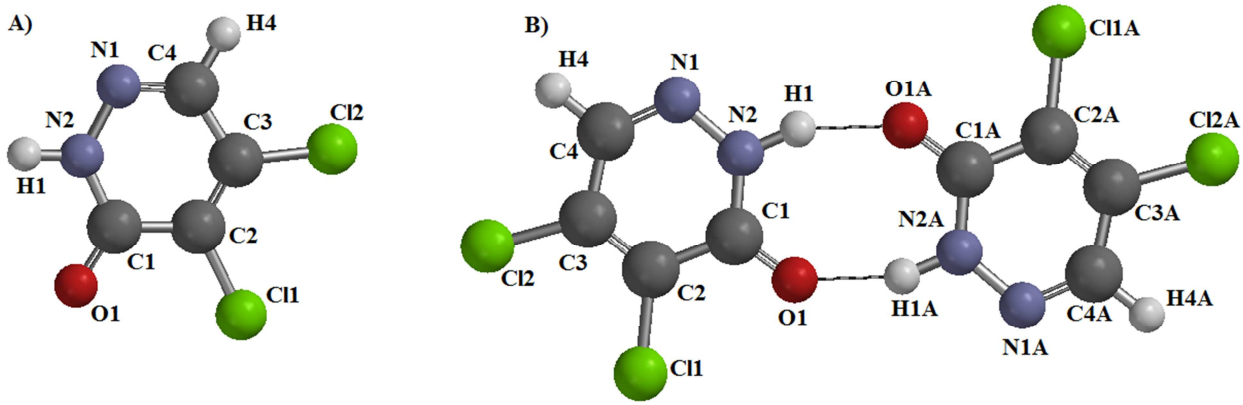

Figure 3. Theoretical structure of the title compound: (a) monomeric and (b) dimeric forms

Table 3. Experimental hydrogen-bond geometry values

D−H···A	Distance (Å)	Angle (º)
N2−H1···O1A	1.894	166.65
C4−H4···O1	2.378	171.18

D: donor; H: hydrogen; A: acceptor.

Calculated bond parameters for monomeric form are consistent with the experimental values, whereas the calculated values for dimeric deviates from experimental values. The reason of these deviations, it can be intermolecular hydrogen bond interactions is given Table 3. Intermolecular interactions values in the title compound are calculated using B3LYP/6-31G(d,p) method and listed in Table 4. Calculated and experimental hydrogen bond interactions values are compatible with each other.

Table 4. Hydrogen-bond geometry values on B3LYP/6-31G(d,p)

D−H···A	Distance (Å)	Angle (º)
N2−H1···O1A	1.807	127.77
C4−H4···O1A	2.574	173.66

D: donor; H: hydrogen; A: acceptor.

Molecular electrostatic potential analysis

The molecular electrostatic potential (MEP), $V(r)$ at a given point r (x,y,z) in the vicinity of a molecule, is defined in terms of the interaction energy between an electrical charge which is generated from the molecule electrons and nuclei and a positive test charge (a proton) located at r [4]. For the system studied, the $V(r)$ values are calculated by the equation [1,4],

$$V(r) = \sum_{A} \frac{Z_A}{(R_A - r)} - \int \frac{\rho(r')}{[r' - r]}\, dr'$$

where Z_A is the charge of nucleus A located at R_A, $\rho(r')$ is the electronic density functional of the molecule, and r' is the dummy interaction variable [4]. To predict the reactive sites of electrophilic and nucleophilic attack for the investigated molecule, the MEP at the B3LYP/6-31G(d,p) optimized geometry of monomeric form was calculated and shown in Figure 4.

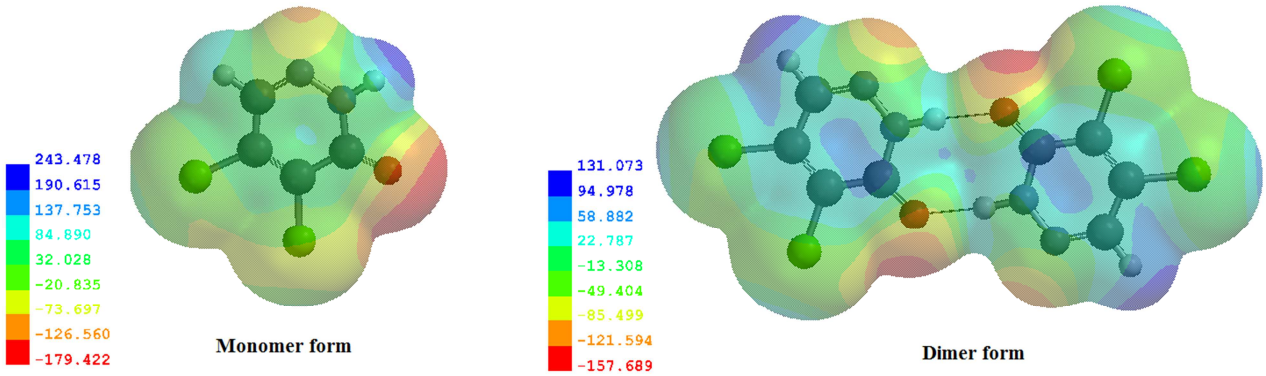

Figure 4. Molecular Electrostatic Potential (MEP) map of the title compound

As seen from Figure 4, the most negative regions are located on the O1 atom which can be considered as possible site for electrophilic attack and its *V(r)* value is -157.689 kJ mol^{-1}. Other negative region is located at N1 atom and *V(r)* value is -121.6 kJ mol^{-1}, that to be related with the electron lone pair at this atom. The MEP is related to the electronic density and is a very useful descriptor for determining sites for electrophilic attack and nucleophilic reactions as well as hydrogen-bonding interactions.

HOMO-LUMO Analysis

The most important orbitals in a molecule are the frontier molecular orbitals, called HOMO and LUMO [4,10]. HOMO implies that the outermost orbital filled by electrons, and behaves as an electron donor while LUMO can be thought as the first empty innermost orbital unfilled by electron and behaves as an electron acceptor [4]. The energy of the HOMO is directly related to the ionization potential and represents the ability of electron giving. But, LUMO energy is directly related to the electron affinity and represents the ability of electron accepting. The formed energy gap between HOMO and LUMO indicates the molecular chemical stability [4,7]. The energy gap between HOMO and LUMO is a critical parameter to determine molecular electrical transport properties. By using HOMO and LUMO energy values for a molecule, chemical hardness-softness, electronegativity and electrophilicity index can be calculated as follows:

$$\mu \sim -x = -\frac{I + A}{2} \ (Electronegativity)$$

$$\eta \sim \frac{I - A}{2} \ (Chemical\ hardness)$$

$$\zeta = \frac{I}{2\eta} \ (Chemical\ Softness)$$

$$\psi = \frac{\mu^2}{2\eta} \ (Electrophilicity\ index)$$

where *I* and *A* is ionization potential and electron affinity, and is I = -E_{HOMO} and A = -E_{LUMO}, respectively [1,4]. Molecules which have a large HOMO-LUMO energy gap are called "hard" and which have a small HOMO-LUMO energy gap are called "soft" [4]. Frontier orbitals (HOMO-LUMO) of the title molecule were calculated using B3LYP/6-31G(d,p) method in gas phase. HOMO-LUMO energy gap values for monomer and dimer forms of this molecule were listed in Table 5.

Table 5. The calculated parameters for the title compound

Parameters	Monomer form (*e*V)	Dimer form (*e*V)
HOMO	-7.0	-6.15
LUMO	-2.30	-2.12
[ΔE] (energy gap)	-4.70	-4.30
μ	4.65	4.13
η	2.35	2.01
ζ	1.48	1.52
ψ	4.60	4.24

The gap energy of the one electron excitation from HOMO to LUMO for monomer and dimer form was calculated about -4.7 *e*V and -4.3 *e*V, respectively. This large HOMO-LUMO gap is an indication of good stability and a high

chemical hardness for the title compound. For monomer and dimer form, 3D plots of highest occupied molecular orbital (HOMO) and lowest unoccupied molecular orbitals (LUMO) were shown in Figure 5.

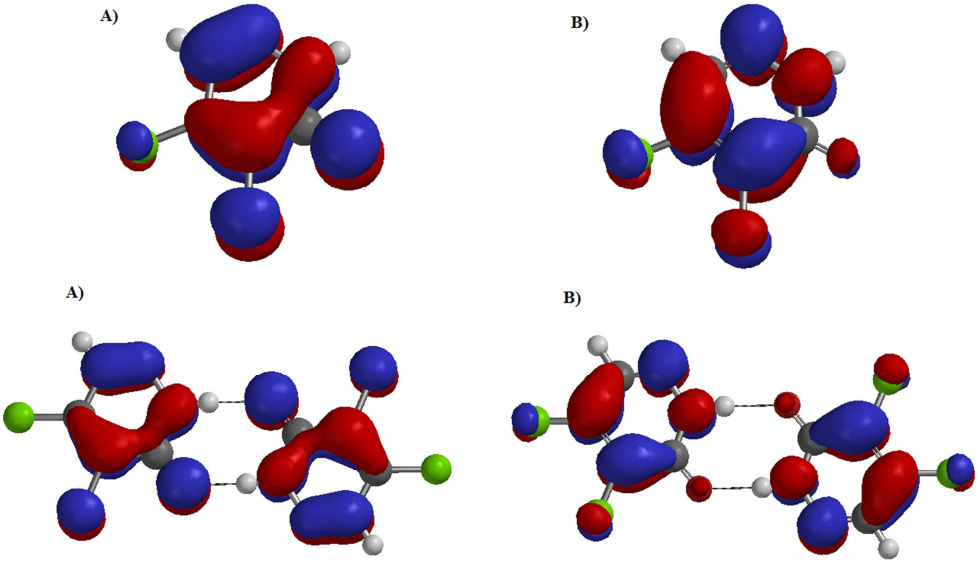

Figure 5. For the title compound 3D plots of (a) HOMO and (b) LUMO

Statistical Analysis

In general, there is a good correlation index (r^2) between experimental data and theoretical results from B3LYP/6-31G(d,p), but is clearly observed which there is a divergence related with dihedral angles (Figure 6). However, this divergence can be explained through of the X-ray structural analysis, where was observed the presence of a deviation in the molecular plane, leading to difference between the results. Finally, the *ab initio* methods, as B3LYP/6-31G(d,p), may not be to predict these torsion angles.

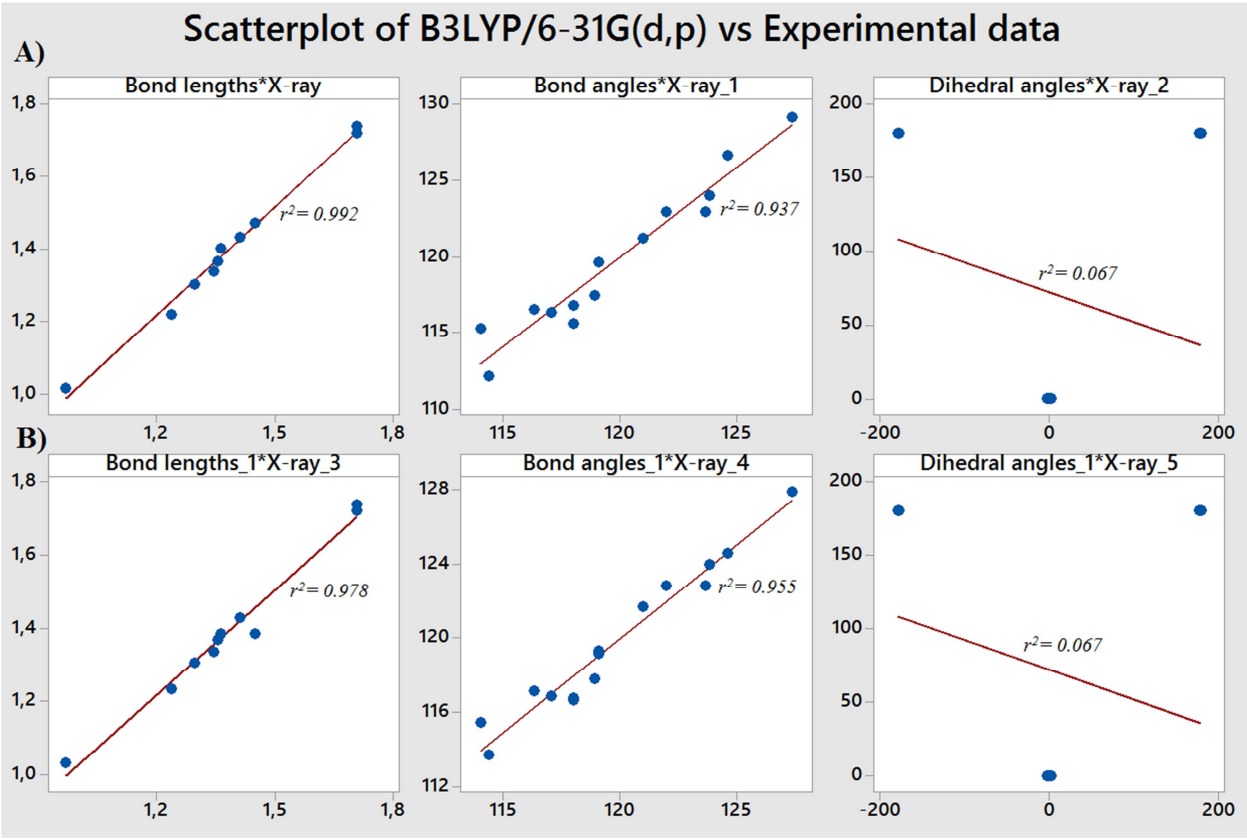

Figure 6. Correlation index (r^2) observed between experimental and theoretical results for the title compound. In (A), results from monomeric structure. In (B), results from dimeric structure

In Figure 7 is shown the structure planarity through of the torsion angles formed by Cl2 – C3 – C2 – C1= 179.67º, Cl1 – C2 – C1 – N2= 179.85º and O1 – C1 – C2 – C3= 179.22º.

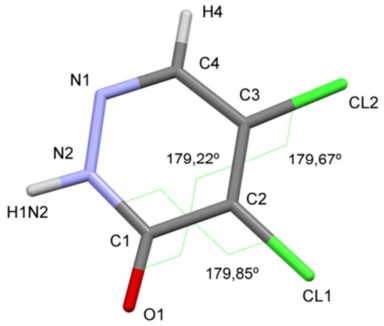

Figure 7. Torsion angles observed by X-ray experiment

CONCLUSION

4,5-Dichloropyridazin-3-(2H)-one has been characterized by using ^{1}H and ^{13}C NMR and X-ray technique experimentally and using B3LYP/6-31G(d,p) method theoretically. Molecular geometry parameters and vibrational frequencies values were calculated using B3LYP/6-31G(d,p) method form monomeric and dimeric form of the compound. Calculated bond lengths values in the monomeric form were found to be more compatible with experimental data, but calculated bond angles showed great accuracy in dimeric form. However, the B3LYP/6-31G(d,p) not was capable to predict torsion angles at pyridazine ring. The MEP map shows that the negative potential sites are around the hydrogen atoms. These sites give information about the region from where the compound can have intermolecular interactions. For monomer and dimer form, HOMO-LUMO energy gap of the molecule are -4.7 *e*V and 4.3 *e*V, respectively. This large HOMO-LUMO gap is an indication of good stability and a high chemical hardness for the title compound.

Acknowledgements
The authors acknowledge the Brazilian National Research Council (CNPq), FAPEAL and CAPES for their financial support in the form of grants and fellowship awards.

REFERENCES

[1] D Singh; AK Ojha; W Kiefer; RK Singh. *Vib. Spectrosc.*, **2009,** 49(2), 242–250.
[2] H Soscún; Y Bermúdez; O Castellano; J Hernández. *Chem. Phys. Lett.*, **2004,** 396(1–3), 117–121.
[3] D Podsiadła; O Czupiński; M Rospenk; B Kosturek. *Vib. Spectrosc.*, **2012,** 59, 47–58.
[4] C Alaşalvar; MS Soylu; H Ünver; NO İskeleli; M Yildiz; M Çiftçi; E Banoğlu. *Spectrochim. Acta A Mol. Biomol. Spectrosc.*, **2014,** 132, 555–62.
[5] A Zarrouk; B Hammouti; H Zarrok; R Salghi; M Bouachrine; F Bentiss; SS Al-Deyab. *Res. Chem. Intermed.*, **2012,** 38(9), 2327–2334.
[6] S Berthel; M County; N Haynes; R Orange; L McDermott; E Windosr; Y Quian; R Sarabu; N Scott; J Tilley. *US Patent App*., **2009**.
[7] Spartan, Model homepage for windows, available at: *http://www.wavefun.com/products/windows/SpartanModel/win_model.html*, acessed in **2015**.
[8] H Zarrok; H Oudda; A Zarrouk. *Der. Pharma. Chem.*, **2011,** 3(6), 576–590.
[9] A Dkhissi; L Adamowicz; G Maes. *J. Phys. Chem. A*, **2000**, 104, 2112–2119.
[10] AD Becke. *Phys. Rev. A*, **1988,** 38, 3098–3100.
[11] SR Salman. *Chem. Mat. Res.*, **2014,** 6(4), 53–60.
[12] F Bentiss; F Gassama; D Barbry; L Gengembre; H Vezin; M Lagrenée; M Traisnel. *Appl. Surf. Sci.*, **2006,** 252, 2684–2691.
[13] A Khadiri; R Saddik; K Bekkouche; A Aouniti; B Hammouti; N Benchat; M Bouachrine; R Solmaz. *J. Taiwan Inst. Chem. Eng.*, **2015,** 000, 1–13.
[14] EnrafNonius. Kappa CCD Operation Manual, **2001**.
[15] GM Sheldrick. Shelx97 program, **1998**.
[16] LJ Farrugia. Ortep-3 for windows, **2011**.
[17] C Cason. POv-Ray for windows, **2011**.
[18] C Groom. The Cambrigde Crystallographic Data Centre, **2011**.